Minimization of dopant-induced random potential fluctuations in sawtooth doping superlattices

E. F. Schubert and T. D. Harris
AT&T Bell Laboratories, Murray Hill, New Jersey 07974

J. E. Cunningham
AT&T Bell Laboratories, Holmdel, New Jersey 07733

(Received 30 August 1988; accepted for publication 19 September 1988)

Potential fluctuations due to random dopant distribution are estimated in a doping superlattice for different doping profiles. It is shown that statistical potential fluctuations are minimized by employing a doping profile consisting of a train of δ functions, which result in sawtooth-shaped band edges. Clearly resolved quantum-confined optical absorption and luminescence transitions are observed in this improved doping superlattice structure. The sawtooth superlattice provides the basis for a novel GaAs technology which is suited to operate in the minimum dispersion region of silica fibers at a wavelength of $\lambda = 1.3\ \mu$m.

Doping superlattices were proposed nearly 20 years ago[1] and consist of alternating n- and p-type doped layers of an epitaxially grown semiconductor. The periodic potential modulation in doping superlattices, which is due to alternating donor and acceptor charges, is the key feature of doping superlattices and gives rise to a number of intriguing phenomena.[2] The band diagram of the originally proposed structure[1] is shown in Fig. 1 (top) and consists of homogeneously doped layers. A sawtooth-shaped band diagram is obtained if the thickness of the doped layer decreases, such that the dopants are localized on a length scale of the lattice constant.[3,4] The sawtooth structure[5] has been used for several novel device concepts such as stimulated light-emitting diodes[6] or photonic switches.[7]

In this letter we investigate statistical potential fluctuations in doping superlattices. We show that potential fluctuations are minimized in the sawtooth structure. Our theoretical conclusions are supported by experimental absorption and emission experiments, which reveal quantum-confined optical transitions for the first time. We propose the sawtooth structure as the basis of a new GaAs technology, which is expected to operate in the minimum dispersion region of optical silica fibers at $\lambda = 1.3\ \mu$m.

The band diagram of the sawtooth superlattice structure is shown in Fig. 2. Electrons and holes occupy quantized eigenstates of energy E_n^e and E_n^h, respectively. Radiative recombination of energy $\hbar\omega$ occurs in the *undoped regions between the dopant layers*. As shown in Fig. 2, the locations of most radiative recombination processes are the tails of the wave functions beyond the classical turning points (i.e., $z^h > z_{nt}^h$ and $z^e < z_{nt}^e$).

We now calculate the average potential fluctuation induced by random dopant distribution in the doped layer. The *thickness* of the doped layer, z_d, is used as a free parameter. The total amount of dopants (per unit area) N^{2D}, is kept constant, that is,

$$N_{A,D}^{2D} = N_{A,D} z_d = \text{constant}, \qquad (1)$$

where $N_{A,D}$ are the three-dimensional acceptor and donor concentrations. This assumption provides the *same* (maximum) electric field in the homogeneously doped and the δ-doped superlattice.

Figure 3 illustrates the configuration which is used as a basis for the calculation. Radiative recombination occurs in the plane $z = z_p/4$ between the two sheets of donors and acceptors. We will now calculate the *potential fluctuation at the location of recombination* ($z = z_p/4$) *caused by randomly distributed dopants* at $z \cong 0$. Again, the thickness of the doped layer, z_d, is used as a free parameter. The volume element dV_i (shown in Fig. 3) contains

$$N = N_D dV_i = (N_D^{2D}/z_d) dV_i \qquad (2)$$

dopant atoms. The number of impurities within this volume element is assumed to fluctuate according to Poisson statistics; the standard deviation is then given by $\sqrt{N}$. The *charge fluctuation* causes a *potential fluctuation* at $(z,r) = (0,0)$ which can be calculated by means of electrostatic principles. For simplicity, we employ unscreened Coulomb potentials and obtain for the mean potential fluctuation:

$$\sigma_{\phi i} = (e/4\pi\epsilon)\sqrt{(N_D^{2D}/z_d) dr\, r d\phi\, dz}\,(r^2 + z^2)^{-1/2}, \qquad (3)$$

where e is the elementary charge, $dr\, rd\phi\, dz$ is the unit volume shown in Fig. 3, and ϵ is the permittivity of the semicon-

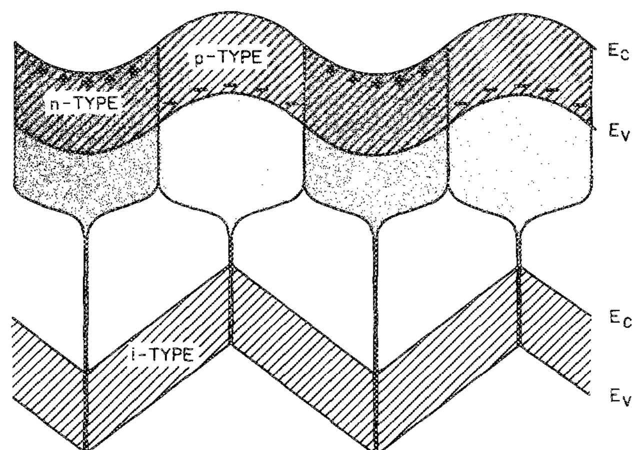

FIG. 1. Schematic energy-band diagram of homogeneously doped superlattice (top) and of a superlattice with very thin doped layers (bottom). Parabolic (top) and V-shaped (bottom) potential wells result from the two doping configurations.

 © 1988 American Institute of Physics

Downloaded 14 Jul 2003 to 128.113.111.105. Redistribution subject to AIP license or copyright, see http://ojps.aip.org/aplo/aplcr.jsp

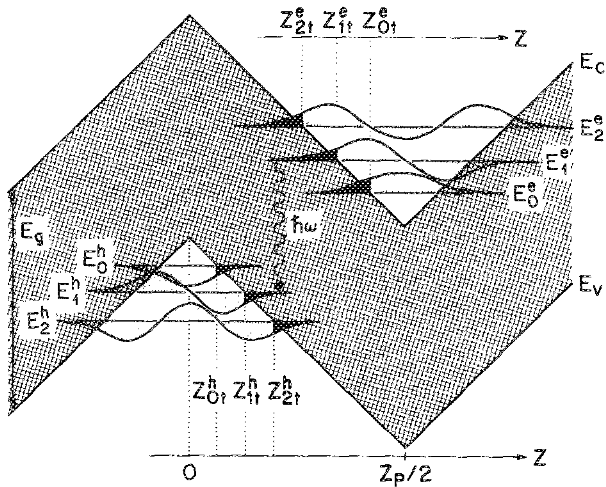

FIG. 2. Schematic illustration of the radiative recombination in a sawtooth superlattice. Recombination occurs predominantly beyond the classical turning points (i.e., $z > z^h_{nt}$ and $z < z^e_{nt}$) in the undoped region between the donor and acceptor sheets. Recombination occurs between electron eigenstate energies (E^e_n) and hole eigenstate energies (E^h_n) with energy $\hbar\omega$; this energy is smaller than the gap energy of the host semiconductor (E_g).

ductor. We further assume that all potential fluctuations are screened out for radii $> r_s$, with $r_s \gg z_p/4$. The total potential can then be obtained by integration over the entire doped layer:

$$\sigma_\phi^2 = 2\pi\left(\frac{N_D^{2D}}{z_d}\right)\left(\frac{e}{4\pi\epsilon}\right)^2\left[\left(\frac{z_p}{4}-\frac{z_d}{2}\right)\times\left(\ln\frac{z_p/4 - z_d/2}{r_s}-1\right)-\left(\frac{z_p}{4}+\frac{z_d}{2}\right)\times\left(\ln\frac{z_p/4+z_d/2}{r_s}-1\right)\right]. \quad (4)$$

We will now try to minimize the potential fluctuations of the doping superlattice to obtain the *optimum dopant distribution* in the superlattice. We use

$$\frac{\partial\sigma_\phi^2}{\partial z_d} = 2\pi\left(\frac{e}{4\pi\epsilon}\right)^2 \times N_D^{2D}\left\{\left[-\frac{z_p/4}{z_d^2}\left(\ln\frac{z_p/4-z_d/2}{r_s}-1\right)+\left(\frac{z_p/4}{z_d}-\frac{1}{2}\right)\frac{-1}{z_p/2-z_d}\right]-\left[-\frac{z_p/4}{z_d^2}\left(\ln\frac{z_p/4+z_d/2}{r_s}-1\right)+\left(\frac{z_p/4}{z_d}+\frac{1}{2}\right)\frac{1}{z_p/2+z_d}\right]\right\}. \quad (5)$$

Minimum potential fluctuations are obtained according to Eq. (5) ($\delta\sigma_\phi^2/\partial z_d = 0$) if the thickness of the doped layer approaches zero, that is, $z_d \to 0$. The doping profile can then be represented by the Dirac–delta function. The magnitude of the potential fluctuation is then given by

$$\lim_{z_d\to 0}\sigma_\phi = \left[2\pi N^{2D}\left(\frac{e}{4\pi\epsilon}\right)^2\left(1-\ln\frac{z_p}{4r_s}\right)\right]^{1/2}. \quad (6)$$

We have recently shown, that dopants can be indeed confined in GaAs with insignificant diffusion of dopants along the growth axis.[4] Thus, improved optical characteristics are expected for the sawtooth structure as compared to the conventional, homogeneously doped superlattice.

The epitaxial GaAs superlattices are grown by gas-source molecular beam epitaxy on a ⟨100⟩ oriented semi-insulating substrate at a substrate temperature of approximately 550 °C. The nominal doping concentration is $N^{2D} = N_D^{2D} N_A^{2D} \cong 1.25\times10^{13}$ cm^{-2} and the period is $z_p = 150$ Å with 10 periods. Absorption measurements are performed on polished, 0.25 cm^2 samples. A dual-beam Perkin–Elmer model 330 spectrophotometer and a variable-temperature cold-finger cryostat are used. Low-temperature

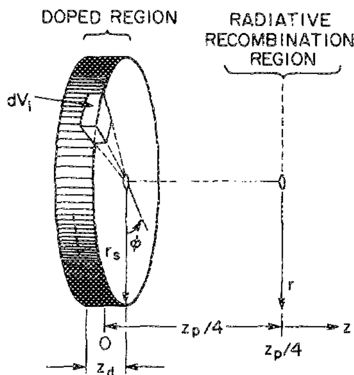

FIG. 3. Schematic illustration of the configuration used to calculate potential fluctuations at $(z,r) = (z_p/4,0)$ caused by dopant density fluctuations in the doped region. Charge fluctuations at radii $r > r_s$ are assumed to be screened out.

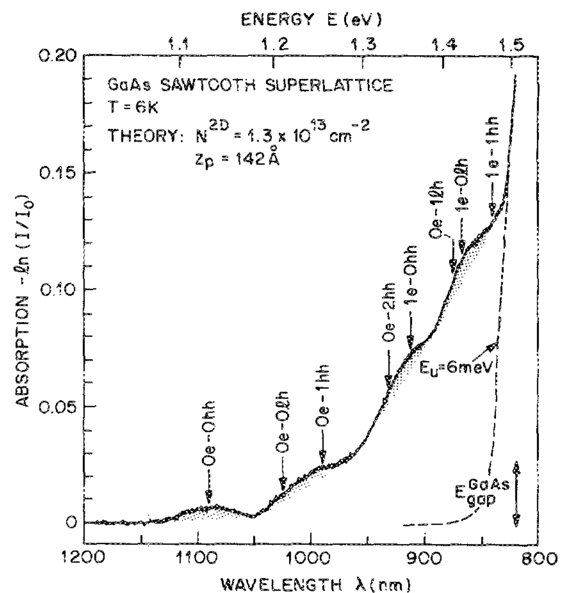

FIG. 4. Low-temperature absorption spectrum of a sawtooth superlattice. Quantum-confined optical transitions at energies below the band gap are identified. Theoretical transition energies are included (arrows).

Downloaded 14 Jul 2003 to 128.113.111.105. Redistribution subject to AIP license or copyright, see http://ojps.aip.org/aplo/aplcr.jsp

photoluminescence measurements are performed at 2 K using the 488 nm line of an Ar^+ ion laser and the 647 nm line of a Kr^+ ion laser for excitation. Luminescence is detected with a Ge pin detector cooled to 77 K and amplified in a phase-sensitive amplifier.

Results of absorption measurements on GaAs sawtooth superlattices measured at $T = 6$ K are shown in Fig. 4. The gap energy of the undoped GaAs substrate corresponds to a wavelength of $\lambda = 820$ nm and is shown by a double arrow. The substrate absorbs light at energies slightly below the fundamental gap; this absorption of bulk material is known as the Urbach tail. We determined the corresponding Urbach-tail energy to be $E_U = 6$ meV for undoped GaAs. A typical absorption spectrum of a GaAs substrate is shown as a dashed curve in Fig. 4.

The absorption spectrum shown in Fig. 4 shows strong absorption below the fundamental gap of GaAs in a range of 400 meV below the band gap of the GaAs host lattice. The most striking aspect of the absorption spectrum are four distinct features: an absorption maximum (peak) at $\lambda = 1090$ nm and three shoulders at wavelength of $\lambda = 1000$, 920, and 865 nm. We attribute the structure to transitions between quantum-confined states in the valence and conduction band. Such quantum-confined interband transitions have not been observed since the original proposal of doping superlattices.

We now compare the experimental absorption data to theoretical transition energies. The calculation using Airy function is described in Ref. 8. The arrows shown in Fig. 2 are calculated energies of quantum-confined transitions. The lowest electron ($n = 0$) to lowest heavy hole ($n = 0$) transition is referred to as *0e—0hh* transition. Very good agreement between calculated quantum-confined transition energies and experimental ones is observed over a wide range of energies. For the calculation a period of $z_p = 142$ Å and a doping concentration of $N^{2D} = 1.3 \times 10^{13}$ cm^{-2} are used to obtain a best agreement between theory and experiment.

The low-temperature photoluminescence spectrum of the sawtooth superlattice is shown in Fig. 5. Three clearly resolved photoluminescence peaks are observed at $\lambda \cong 0.98$, 1.02, and 1.09 μm. Again, we attribute the clearly resolved luminescence peaks to transitions between quantum-confined conduction- and valence-band states. Theoretical transition energies are included as well.

Our absorption and photoluminescence measurements clearly show that the sawtooth structure represents an *ideal* doping superlattice structure due to (i) minimization of undesired potential variations, (ii) large potential modulation, and (iii) small superlattice period. Our improved structure provides the basis of a new GaAs technology that is expected to operate at the dispersion minimum of silica fiber at $\lambda = 1.3\ \mu$m.[9]

In conclusion, we have shown that dopant-induced random potential fluctuations are minimized if the doping profile consists of a δ-function train of n- and p-type dopants. Together with the feasibility of high superlattice potential modulation, and small periods ($z_p \cong 150$ Å), the sawtooth superlattice represents an optimized doping superlattice structure. Experimental evidence for the improvement is

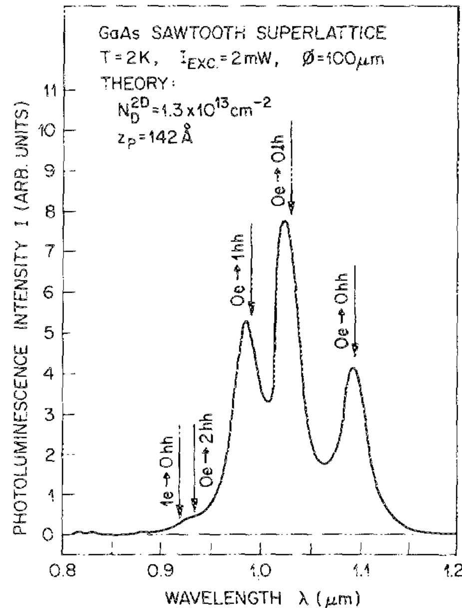

FIG. 5. Low-temperature photoluminescence spectrum of a sawtooth superlattice. Clearly resolved, quantum-confined transitions are identified by comparing them with calculated transition energies.

provided by means of low-temperature absorption and photoluminescence measurements. Clearly resolved quantum-confined transitions are observed in absorption and emission for the first time. The sawtooth superlattice structure provides the basis for a novel GaAs technology which is suited to operate in the minimum dispersion region of silica fibers at a wavelength of $\lambda = 1.3\ \mu$m.

The authors would like to thank T. H. Chiu, L. C. Feldman, A. Ourmazd, S. Schmitt-Rink, and W. T. Tsang for valuable discussions.

[1]L. Esaki and R. Tsu, IBM J. Res. Develop. **14**, 61 (1970); M. I. Ovsyannikov, Y. A. Romanov, V. N. Shabanov, and R. G. Loginova, Sov. Phys. Semicond. **4**, 1919 (1971); Y. A. Romanov, *ibid.* **5**, 1256 (1972); G. H. Döhler, Phys. Status Solidi B **52**, 79 (1972).
[2]See, for example, L. Esaki, IEEE J. Quantum Electronics **22**, 1611 (1986); G. H. Döhler, *ibid.* **22**, 1682 (1986); K. Ploog and G. H. Döhler, Adv. Phys. **32**, 285 (1983).
[3]E. F. Schubert, J. B. Stark, B. Ullrich, and J. E. Cunningham, Appl. Phys. Lett. **52**, 1508 (1988).
[4]Diffusion of Si in GaAs was shown to be irrelevant at low growth temperatures, see E. F. Schubert, J. B. Stark, T. H. Chiu, and B. Tell, Appl. Phys. Lett. **53**, 293 (1988).
[5]E. F. Schubert, Y. Horikoshi, and K. Ploog, Phys. Rev. B **32**, 1085 (1985); E. F. Schubert, J. E. Cunningham, and W. T. Tsang, Phys. Rev. B **36**, 1348 (1987).
[6]E. F. Schubert, A. Fischer, Y. Horikoshi, and K. Ploog, Appl. Phys. Lett. **47**, 219 (1985). A current injection laser with a conventional doping superlattice in the active region was realized by B. A. Vojak, G. W. Zajac, F. A. Chambers, J. E. Meese, and P. E. Chumbey, Appl. Phys. Lett. **48**, 251 (1986).
[7]E. F. Schubert and J. E. Cunningham, Electron. Lett. **24**, 980 (1988).
[8]E. F. Schubert, B. Ullrich, T. D. Harris, and J. E. Cunningham, Phys. Rev. B **38**, 8305 (1988).
[9]In superlattices with longer periods ($z_p = 300$–600 Å) we have observed strong infrared photoluminescence with emission maxima ranging from 1.3 to 1.6 μm.

Downloaded 14 Jul 2003 to 128.113.111.105. Redistribution subject to AIP license or copyright, see http://ojps.aip.org/aplo/aplcr.jsp